Joule

CellPress

Article

Deep neural network battery charging curve prediction using 30 points collected in 10 min

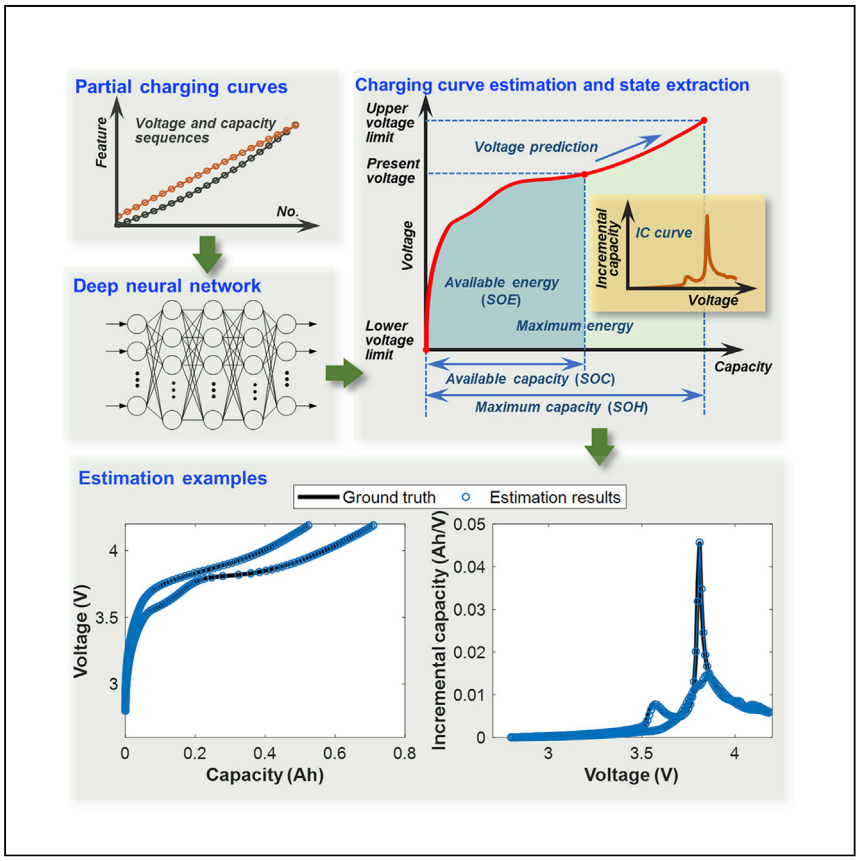

Battery state-of-health estimation plays a critical role in battery management. In this study, a deep-learning approach is proposed to estimate entire charging curves by taking portions of charging curves as input. Therefore, multiple battery states can be determined at different aging levels. Besides, the proposed method can quickly adapt to different batteries without much training effort. The proposed method opens a new way to estimate the aging characteristics of batteries.

Jinpeng Tian, Rui Xiong, Weixiang Shen, Jiahuan Lu, Xiao-Guang Yang

rxiong@bit.edu.cn

Highlights

A deep-learning approach is proposed to estimate charging curves of batteries

The proposed method accepts flexible input collected during daily charging

Key states and even incremental capacity curves can be accurately derived

The proposed method can quickly adapt to new different batteries

Tian et al., Joule 5, 1521–1534
June 16, 2021 © 2021 Elsevier Inc.
https://doi.org/10.1016/j.joule.2021.05.012

Joule

CellPress

Article

Deep neural network battery charging curve prediction using 30 points collected in 10 min

Jinpeng Tian,[1] Rui Xiong,[1,3,*] Weixiang Shen,[2] Jiahuan Lu,[1] and Xiao-Guang Yang[1]

SUMMARY

Accurate degradation monitoring over battery life is indispensable for the safe and durable operation of battery-powered applications. In this work, we extend conventional capacity degradation estimation to the estimation of entire constant-current charging curves. A deep neural network (DNN) is developed to estimate complete charging curves by featuring small portions of the charging curves to form the input. We demonstrate that the charging curves can be accurately captured with an error of less than 16.9 mAh for 0.74 Ah batteries with 30 points collected in less than 10 min. Validation based on batteries working at different current rates and temperatures further demonstrates the effectiveness of the proposed method. This method also enjoys the advantage of transfer learning; that is, a DNN trained on one battery dataset can be used to improve the curve estimation of other batteries operating under different scenarios by using few training data.

INTRODUCTION

Lithium-ion batteries have been adopted in a wide spectrum of applications, ranging from electric vehicles to portable electronic devices. One of the longstanding blocks that jeopardize the management of lithium-ion batteries is health degradation, which is primarily reflected by capacity loss.[1,2] Accurate assessment of the maximum battery capacity plays a pivotal role in designing battery-management strategies and planning battery maintenance.

The assessment of maximum battery capacity requires a complete charging/discharging curve spanning from the lower to the upper voltage limits.[3] In applications such as electric vehicles and smartphones, complete charge curves are rarely available. Instead, the charging process can start at various states (or voltages) and might not end in a fully charged state. The analysis of real-world battery-management data in electric vehicles reveals that only pieces of charging/discharging curves are recorded by a battery-management system (BMS).[4] In response to this issue, a range of maximum capacity estimation methods has been proposed in previous studies.[5–7] Generally, the features derived from measured battery signals are fed into regression algorithms to predict the maximum battery capacity. Zhang et al.[8] incorporated impedance spectra into Gaussian process regression (GPR) for maximum battery capacity estimation and lifetime prediction. This method outperforms a conventional approach based on multiple handpicked features.[9] However, the measurement of impedance spectra requires additional hardware and is computationally expensive.[10] In reality, BMSs typically sample charging/discharging current and voltage of batteries. The controllable charging protocols[11] can provide more consistent input to machine-learning approaches than unpredictable dynamic discharging profiles.[12] Therefore, Weng et al.[13]

Context & scale

Battery health monitoring (BHM) is one of the most crucial issues to ensure the safe and durable operation of battery-powered applications. A key challenge to BHM is to estimate the maximum battery capacity. However, maximum battery capacity as a scalar only provides limited information about battery states. In this work, we propose to use a deep neural network (DNN) to estimate entire charging curves. The DNN takes as input only small portions of charging curves. In this way, key battery states such as capacity and energy can be extracted. We also demonstrate that the DNN can adapt to different batteries working in different conditions. Therefore, the training effort can be significantly reduced when developing a DNN for different battery datasets.

derived the incremental capacity (IC) curves from constant-current charging curves and found that the height of IC peaks is a monotonic function of maximum battery capacity, which can be used to determine capacity loss. Similar features include the location of IC peaks and statistical indicators.[14] Nevertheless, IC curves require differentiation of charging curves, which inevitably amplifies sampling noise. Follow-up studies improved these methods by substituting these handpicked features with directly sampled data, whereby machine-learning algorithms are used to estimate maximum battery capacity by feeding in specific parts of constant-current charging curves.[15,16] However, they require a specific voltage window to extract feasible features, which might not be flexible enough to fulfill capacity estimation in various operating scenarios.

Another challenge that remains unsolved is the estimation of battery states over battery life. Although maximum battery capacity has been successfully estimated, as a scalar, it can only provide limited information about battery states. Other methods are required to estimate fast-changing states such as state of charge (SOC)[17] and state of energy (SOE)[18] by assuming that the maximum battery capacity is already known. A few estimation methods[19,20] have been proposed to simultaneously estimate several states, but they were rarely designed or validated at a battery life scale. These facts necessitate one estimation approach that can comprehensively reflect states by using signals obtained from daily battery operation.

In this study, we show that the complete constant-current charging curves can be estimated by using a piece of the charging curve as the input of a deep neural network (DNN). Key states can then be readily derived from the estimated entire charging curve, as schematically illustrated in Figure 1. Our method improves conventional state estimation methods from three aspects.

First, we estimate the entire constant-current charging curves, as demonstrated in Figure 1C. Charging curves can reflect the available battery capacity at different voltages. In this regard, the maximum capacity, which is usually used to define the state of health (SOH), is only the capacity at the upper voltage limit. As a result, the available battery capacity can be readily estimated as a function of voltage, rather than resorting to the estimation of SOC, which is defined as the ratio of the available capacity to maximum capacity.[17,21] We can also extract energy-related states from charging curves. The maximum energy is the integral of capacity over the entire allowable voltage range, and it is directly related to energy consumption[22] or the maximum driving range of an electric vehicle.[23] The energy at a given voltage can also be computed without estimating SOE.[24] Furthermore, we can predict battery voltage during charging to assess the state of power (SOP)[25] and derive the IC curves for a more in-depth analysis of battery-aging mechanisms.[26]

Second, in contrast to conventional methods that require input data collected in specific voltage/SOC ranges,[9,15,16] our method can use data collected in different voltage windows as input. As shown in Figure 1A, we can use voltage and capacity sequences collected from any part of the charging curve as the input to the DNN. Therefore, the input can be readily extracted from incomplete charging processes that might not begin or end at the battery voltage limits, making input data more flexible and easier to obtain in the context of real-world battery management.[4] We show that the entire charging curves can be accurately estimated with less than 10 min of charging data. Such flexibility favors applications of the proposed method in battery systems operating under various conditions.[27]

[1]Department of Vehicle Engineering, School of Mechanical Engineering, Beijing Institute of Technology, Beijing 100081, China

[2]Faculty of Science, Engineering and Technology, Swinburne University of Technology, Hawthorn, VIC 3122, Australia

[3]Lead contact

*Correspondence: rxiong@bit.edu.cn

https://doi.org/10.1016/j.joule.2021.05.012

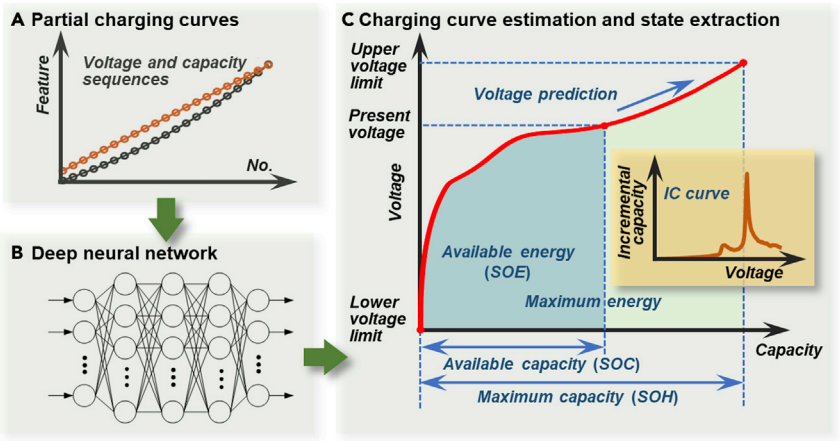

Figure 1. Schematic diagram of the charging curve estimation method

Partial charging curves are used as the input of a DNN, which outputs the complete charging curve. Key states can then be derived from the charging curve.

Third, the transfer-learning technique enables the fast development of a new DNN for different batteries with a less computational burden and higher accuracy. We demonstrate that a pre-trained DNN based on one dataset can quickly adapt to other datasets where different batteries undergo different aging tests. In this way, testing and training efforts can be reduced while the estimation accuracy and reliability are still ensured.

Method overview

In a constant-current charging process, the voltage $V(t)$ and current $I(t)$ are sampled by a BMS. Battery capacity Q is then computed as a function of voltage:

$$Q(V) = \int_{V(\tau)=V_{lower}}^{V(\tau)=V} |I(\tau)|d\tau \qquad \text{(Equation 1)}$$

where V_{lower} denotes the lower voltage limit. A charging curve can be described by $Q(V)$, which is discretized by giving a voltage step ΔV. $Q(V)$ is then sampled at $\boldsymbol{V} = [V_{lower}, V_{lower}+\Delta V, \ldots, V_{lower}+N\Delta V]$, where $N = (V_{upper} - V_{lower})/\Delta V$, and V_{upper} denotes the upper voltage limit. Thus, the entire charging curve is encoded into a $2\times(N+1)$ matrix $[\boldsymbol{V}; \boldsymbol{Q}(\boldsymbol{V})]$. As the charging process is usually incomplete in many scenarios,[16] this study aims to estimate $\boldsymbol{Q}(\boldsymbol{V})$ with only a portion of a charging curve, i.e., the input is $\boldsymbol{H} = [\boldsymbol{V}(s, s+1, \ldots, s+a); \boldsymbol{Q}(\boldsymbol{V}(s, s+1, \ldots, s+a)) - \boldsymbol{Q}(\boldsymbol{V}(s-1))]$, $(1 \le a \le N-1,\ 2 \le s \le N-a+1)$. In this way, $(N-a)$ input samples can be collected from a charging curve, and their corresponding estimation target is the entire charging curve $\boldsymbol{Q}(\boldsymbol{V})$. The input $\boldsymbol{H}$ consists of the voltage and capacity sequences and the voltage sequence indicates the location of the sampled capacity sequence, which vary at different battery-aging levels. Besides, the sampling of the input capacity sequence is not dependent on a complete charging curve. Instead, the ampere-hour counting starts and sets the capacity Q to 0 when the voltage reaches $V(s-1)$. Afterwards, capacity Q is computed at the given voltage series until the battery is charged to $V(s+a)$. Therefore, the input can be readily extracted from incomplete charging processes which might not begin or end at the battery voltage limits, making input data more flexible and easier to obtain in the context of real-world battery management.[4] We intend to develop a DNN which takes the input $\boldsymbol{H}$ with any possible s as the input to output the entire $\boldsymbol{Q}(\boldsymbol{V})$ to restore the entire charging curve at unknown aging states.

RESULTS

Battery degradation data

The Oxford Battery Degradation Dataset 1, which is publicly available,[28] is primarily adopted for the development and validation of the proposed method. It comprises data collected from degradation tests on eight 0.74 Ah pouch cells, whose voltage window ranges from 2.7 to 4.2 V. Periodic 1 C constant-current charging curves at 40°C are adopted to simulate daily battery charging at different aging states, as shown in Figure S1. Detailed specifications and loading profiles of the batteries can be found in Note S1. As some batteries do not exactly reach the lower or upper voltage limit in some cases, the discretized charging curve $\boldsymbol{Q}(V)$ is extracted from the voltage range between 2.8 and 4.19 V by using linear interpolation with a sampling interval of $\Delta V = 10$ mV, resulting in an output vector containing 140 elements. The capacity variation out of this voltage window is negligible. The training dataset consists of the data from the first six batteries, and the data from the remaining two batteries comprise the test dataset.

Curve estimation

We first consider a case of charging-curve estimation given an input window length of 300 mV. The root mean squared error (RMSE) in terms of charging-curve estimation based on the test dataset is computed as The root mean squared error (RMSE) in terms of charging curve estimation based on the test dataset is computed as $RMSE = \sqrt{\frac{1}{N+1}\sum_{i=1}^{N+1}(Q(V(i)) - \widehat{Q}(V(i)))^2}$, where Q is the estimation results of Q., where $\widehat{\boldsymbol{Q}}$ is the estimation results of $\boldsymbol{Q}$. The results are plotted in Figure 2A as a function of the starting voltage of the input sequence and observed maximum capacity extracted from the sampled charging curve, i.e., the battery capacity at 4.19 V. Over the entire battery lifetime, the proposed method can estimate the complete charging curves with RMSEs of less than 16.9 mAh (2.28% of the nominal capacity of 0.74 Ah) and the average RMSE of 4.491 mAh. To visually examine the estimation results, the best and worst curve estimation examples at the first and last cycles in the test dataset are plotted in Figure 2C. One can find that the estimation results are consistent with the starting voltages of the input covering the entire battery voltage range. In addition to charging-curve estimation, the corresponding IC curves are also derived by using $IC(k) = \frac{Q(V(k+1)) - Q(V(k))}{\Delta V}, (1 \leq k \leq N)$; the results are plotted in Figure 2D. IC curves have been reported to be a versatile tool for diagnosing battery-aging mechanisms. For instance, the shrinkage and shift of IC peaks can reflect the loss of active materials and lithium inventory.[26,29–31] In our estimation results, both the best and worst estimation results follow the variation of the IC curves closely and can accurately portray the IC peaks, offering fundamental insights into battery degradation. Therefore, we no longer need IC analysis for aging diagnosis or aging estimation. Instead, the entire IC curves can be constructed by using only a portion of the charging data spanning a 300-mV range. Figure 2A also reveals that the DNN generally has the best estimation performance when the input sequence starts at approximately 3.5 – 3.8 V, as indicated by the deep color. This can be explained by the IC curves shown in Figure 2D. Salient changes in the charging curves are converted to a dominant IC peak showing a clear decreasing trend. This region is most informative in terms of battery degradation. However, the region where the dominant IC peak appears accounts for most of the capacity. A 300-mV voltage window in this region can last up to 34.48 min (Figure 2B). Thus, it is relatively less accessible in daily applications. At low or high starting voltages, the duration is significantly reduced; for example, at an initial voltage of 2.8 V, the duration can be as short as 9.45 min. In this region, the DNN still gives reliable estimations even though their charging curves or IC curves are hard to distinguish visually.

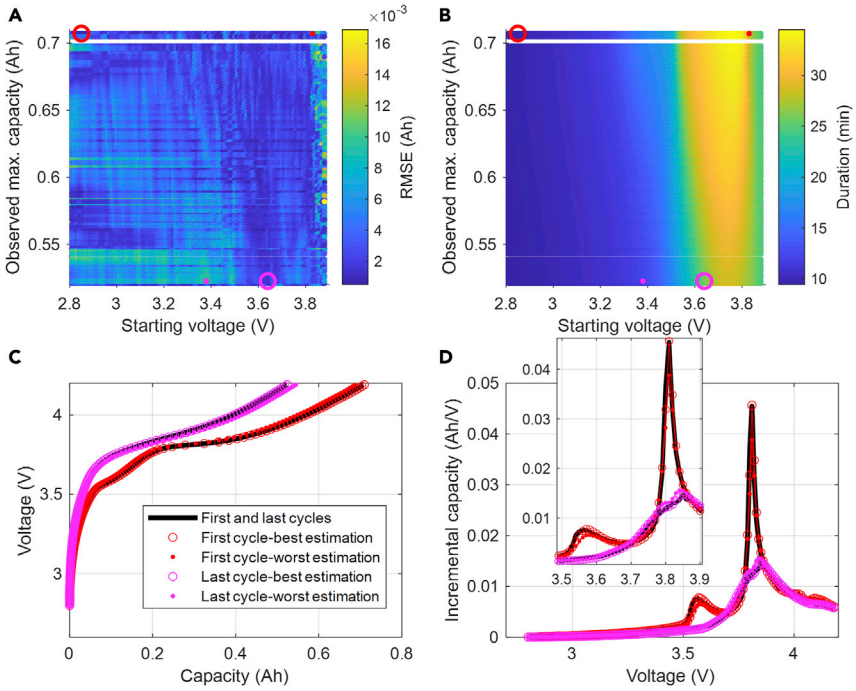

Figure 2. Curve estimation results

(A) RMSE of charging-curve estimation for the Oxford dataset.

(B) The duration to collect the input sequence. In (A) and (B), the x axis is the starting voltage of the input sequence and the y axis is the corresponding observed maximum capacity, representing different aging states. The color indicates the RMSE and duration, respectively.

(C) Examples of the best and worst curve estimation results at the first and last cycles in the test datasets.

(D) IC curves of the two examples. The locations of the two examples in (C) and (D) are marked in (A) and (B).

Maximum capacity and energy estimation

The results in Figure 2 demonstrate that we can accurately estimate battery capacity as a function of the charging voltage, i.e., $\boldsymbol{Q}(\boldsymbol{V})$. On the other hand, we can also compute battery energy at a given voltage, i.e., $\boldsymbol{E}(\boldsymbol{V})$. It is computed as an integral over the entire charging/discharging process:

$$E(V) = \int_{V(\tau)=V_{lower}}^{V(\tau)=V} |V(\tau)I(\tau)|d\tau \qquad \text{(Equation 2)}$$

Some states of interest can then be extracted from the estimated charging curves, such as the maximum battery capacity, which usually defines SOH[32] and maximum energy. These two quantities are extracted as the two examples to demonstrate the capability of the proposed method, and their estimation errors are plotted in Figures 3A and 3B; the estimation error regarding maximum battery capacity and energy is normalized by the nominal capacity (0.74 Ah) and the maximum energy (2.698 Wh) of the first cycle, respectively. Using data starting at any voltage, the proposed method can estimate the maximum capacity with the absolute value of the estimation error below 4.12% and with an average error of 1.11%. Such accuracy is competitive with the methods focusing only on the estimation of maximum battery capacity.[33] To demonstrate this, we adopt three widely used machine-learning techniques as baseline methods, namely random forest (RF),[16] support vector regression (SVR)[34] and GPR.[15] Each method uses input data that are identical to the proposed

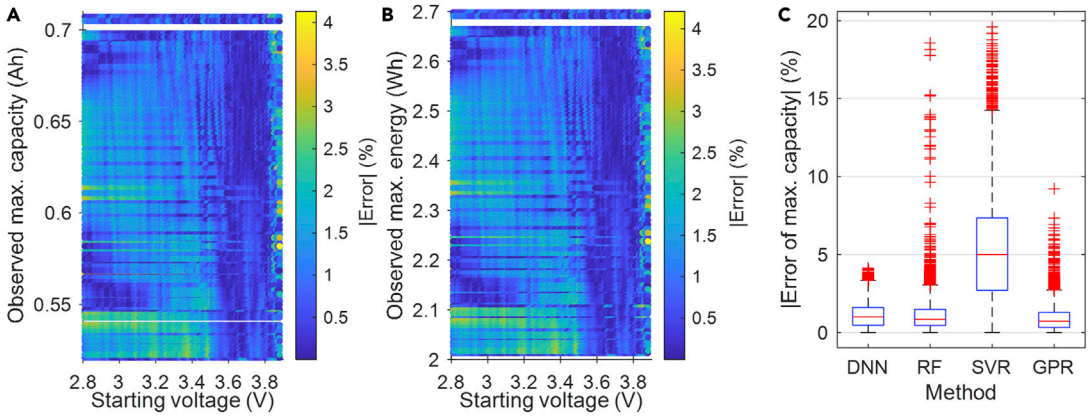

Figure 3. The absolute value of the estimation error

(A and B) Shown is the (A) maximum capacity and (B) maximum energy extracted from the estimated charging curves.

In (A) and (B), the x axis is the starting voltage of the input sequence, and the y axis is the observed maximum capacity/energy, representing different aging states. The maximum capacity error and maximum energy error are normalized by the nominal capacity (0.74 Ah) and the maximum energy of the first cycle (2.698 Wh), respectively.

(C) Error distribution of the estimation of the maximum capacity. RF, SVR and GPR are adopted as baseline methods.

DNN. These conventional methods[15,16,34] can only estimate the maximum battery capacity instead of an entire charging curve. The distribution of their estimation errors is plotted in Figure 3C. As can be noted, the maximum capacities extracted from the estimated charging curves show high accuracy with the smallest maximum error and generally small error distribution. RF and SVR fail to provide reliable estimation with their maximum estimation error over 15%. In contrast, GPR has better overall performance, but the maximum estimation error still reaches 9.22%. In summary, the estimated entire charging curves can realize reliable extraction of the maximum capacities. A detailed description of the three estimation methods can be found in Note S2.

As mentioned earlier, the maximum battery capacity is only the capacity at the upper voltage limit. In this regard, our model outputs the available capacity at each voltage. Thus, one can easily estimate the available capacity once the charging voltage is recorded during the charging process. Afterwards, the variation of the available capacity during battery operations can be computed through ampere-hour counting.[35] This indeed circumvents the issue in SOC estimation, which usually assumes the maximum battery capacity as a known parameter and is usually susceptible to low-voltage modeling accuracy[36] or inconsistent dynamic profiles.[35] Besides, the flexible input of the curve estimation also makes the calibration of the available capacity accessible. In addition to capacity in Ah, the maximum energy in Wh can also be extracted. It reflects the battery energy, which directly determines many energy-related quantities, such as the driving range of electric vehicles and electricity bills of a household. Such information cannot be directly reflected by conventional Ah-only estimation as energy is correlated not only to capacity but also to voltage. An example showing the difference between capacity loss and energy loss is given in Figure S2. Experimental studies have demonstrated that lithium-ion batteries typically have an energy efficiency of greater than 90%.[37] Given this, the maximum energy computed during the charging process provides a reference for the energy that a battery can release. Similar to capacity estimation, once we know the battery voltage, the stored battery energy can be estimated. The maximum and average absolute energy estimation errors of the proposed method are 4.21% and 1.15%, respectively.

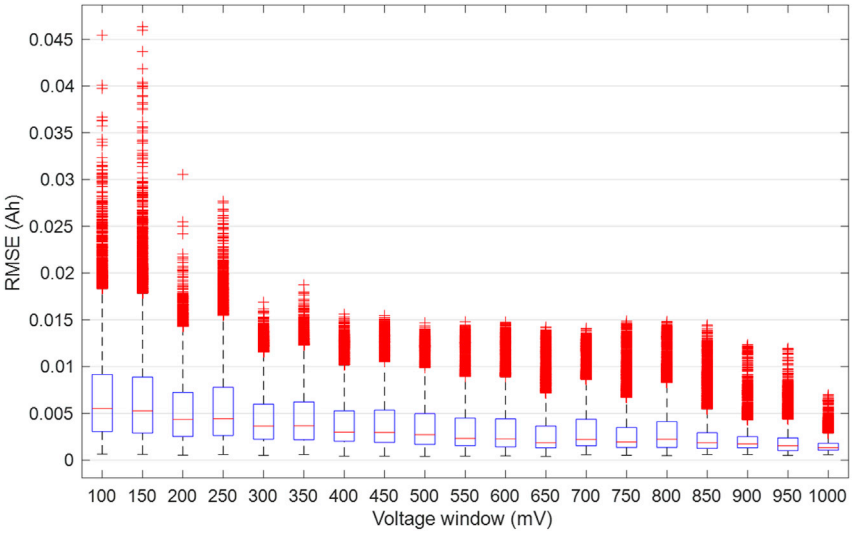

Figure 4. The influence of the voltage window length on the accuracy of curve estimation

Influence of the input length

The influence of the window length is investigated by varying the window length from 100 to 1,000 mV with steps of 50 mV. Each case includes a model intensively trained for the maximum number of 50,000 epochs. The distribution of the curve estimation error is plotted in Figure 4. It can be noticed that a length of 100 mV (10 points only) is sufficient to make an accurate estimation with the RMSE below 0.02 Ah in most cases. Generally, a large window can reduce the overall RMSE, eliminate the outliers, and narrow the error distribution. Its cost is the increased duration to acquire the input sequence. However, the accuracy improvement induced by increasing the window length is limited for a window length over 300 mV. One might need to find out a suitable window length according to a specific scenario to balance the estimation accuracy and the sampling duration.

Curve estimation at different temperatures and current rates

The current rate and ambient temperature play a critical role in battery performances. In particular, charging at a high current rate and a low temperature has been reported to trigger Li plating, leading to fast degradation.[38] To explore the capability of the DNN to estimate the charging curves in such a case, eight 2.4 Ah 18650 batteries (LR1865SZ in Table 1) were tested at high charging-current rates at 25°C. They were divided into two groups and cycled for 100 times at a constant-current charging rate of 2 and 3 C, respectively. All batteries experienced a significant capacity drop. The details regarding the dataset can be found in Note S3.

After the training and testing settings in the above sections, we used a 300-mV voltage window to sample the charging data as the input to predict the entire charging curves. The RMSEs in terms of curve estimation are plotted in Figure 5. As can be noted, the DNN maintains satisfactory performance over battery degradation with most of the estimation RMSEs within 0.04 Ah. The maximum prediction RMSE is 0.18 and 0.1 Ah for batteries charged at 2 and 3 C, respectively. The DNN shows consistent performance in both cases; this implies the DNN can work effectively at different temperatures and current rates even when the batteries significantly degrade.

Table 1. Additional battery datasets adopted for method validation

Dataset	Materials	Nominal capacity	Current rates	Temperature
LR1865SZ	$LiCoO_2$ +$LiNi_{0.5}Co_{0.2}Mn_{0.3}O_2$ cathode and graphite anode	2.4 Ah	2 C, 3 C	25°C
NASA	not reported	2.1 Ah	1/2.1 C	40°C
CALCE	$LiCoO_2$ cathode	1.1 Ah	1 C	20°C–25°C

Fast curve estimation for different batteries

In the context of battery management, developing a brand new DNN can be expensive in terms of cost and time, as it requires extensive battery degradation tests for collecting new training data. On the other hand, real-world data are usually sparse and incomplete,[4] which poses a significant challenge in DNN development. Given this, we expect degradation data collected from one batch of batteries can facilitate the development of a new DNN for different batteries with a small amount of additional data, although working loads and even battery types might be different. The transfer-learning feature of DNNs is an effective tool to fulfill this task.[39] The transfer learning can resort to the "similar knowledge" learned from the source dataset to improve its performance on the target dataset, reduce the required data amount, and save computational resources. In the context of curve estimation, this similar knowledge is supported by two facts. First, although batteries might have different specifications such as nominal capacities and electrode chemistries, their basic working principles are similar. Second, although the current rates and ambient temperatures might be different, the studied charging curves are obtained under constant current, leading to similar voltage profiles.

Here, we explore the transfer-learning capability of the DNN on the basis of two publicly available battery degradation datasets. The trained DNN based on the Oxford dataset is fine-tuned to adapt to the batteries RW21~RW28 in the NASA dataset[40,41] and the batteries CS2-35~CS2-38 in the Center for Advanced Life Cycle Engineering (CALCE) dataset,[42,43] rather than developing a new DNN. The NASA and CALCE batteries are significantly different from the Oxford batteries in terms of the chemistries and working conditions (see Table 1). The constant-current discharging data are adopted to extract the curves to demonstrate the applicability of the proposed method by using either charging or discharging data. For the NASA batteries, the voltage range for estimation is determined to be from 3.21 to 4.05 V, yielding a regression target of a length of 85. For the CALCE batteries, the voltage range for curve extraction is set to be from 2.71 to 4.18 V, and thus one curve is encoded into 148 elements. A detailed description of the two NASA and CALCE datasets can be found in Note S4.

In the transfer-learning approach, the final output layer of the trained DNN for the Oxford batteries is replaced by a new dense layer, whose number of neurons agrees with that of elements in an extracted charging curve. Afterwards, the DNN is trained on the data selected from the NASA and CALCE datasets, respectively. As discussed above, we expect a fast training process with a small number of training samples. Therefore, the training dataset of NASA batteries comprises only 21 curves collected only from the batteries RW21 and RW22, whereas the test dataset contains the remaining six batteries. Similarly, 21 curves are evenly sampled over the cycling test of the CS2-36 battery.

We scale down the battery capacity according to the ratio of nominal capacities during estimation, i.e., $Q_{new}(V) = 0.74/Q_{norm} \times Q(V)$, where Q_{norm} denotes the

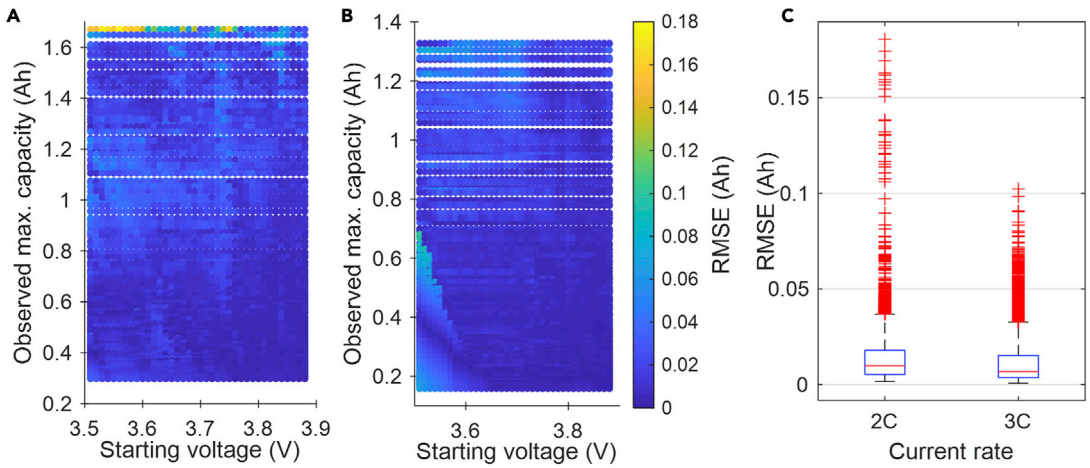

Figure 5. RMSE of charging-curve estimation for the LR1865SZ batteries
(A and B) Batteries cycled at 2C (A) and 3C (B) rates.
(C) The distribution of RMSEs in (A) and (B).

nominal capacity of different battery types. This helps alleviate the underlying issue caused by inconsistent nominal capacities of different battery types, and we can easily obtain $Q(V)$ in reverse. As the training process is random to some extent, both the transfer-learning and direct-training approaches are implemented 20 times with a maximum number of 5,000 epochs. The RMSE distribution in terms of curve estimation are compared in Figures 6A and 6B for the NASA and CALCE batteries, respectively. In both cases, the transfer-learning capability of the proposed method is able to give more reliable estimation results as the RMSEs are more centralized near 0. Also, fewer outliers can be observed. Figures 6C and 6D reveal that the 20 models fine-tuned through transfer learning generally have shown better performances with most of the average RMSEs below those of the counterparts obtained by direct training. Besides, less dispersion can be observed, indicating consistent training performance. The heatmaps showing the RMSEs of each DNN can be found in Note S5. In particular, as CALCE batteries underwent nonlinear capacity loss which is usually ascribed to sudden Li plating[44] (see Figure S6), the proposed method is robust against varying degradation mechanisms.

It should be noted that transfer learning still faces some underlying challenges. As discussed by Pan et al.,[39] the basis of transfer learning is the similarity between the source and target datasets. If the similarity between two datasets is not sufficient, the effectiveness of transfer learning will be diminished; this effect is referred to as "negative transfer." More advanced transfer-learning techniques are being developed to resolve this issue, as demonstrated by Tan et al.[45]

Rationality toward real-life applications and outlooks

Different from conventional studies,[5–7] which only estimate the maximum capacity to reflect battery health, the proposed method enables the accurate estimation of entire charging curves by using flexible charging data collected within a small voltage window. As conventional studies using charging data to estimate the maximum capacity have been intensively used, the proposed method is promising to be implemented for battery management, especially in a cloud BMS,[46] to enable the reflection of the high-dimensional characteristics of batteries, which coincides with the concept of battery "digital twin[47]."

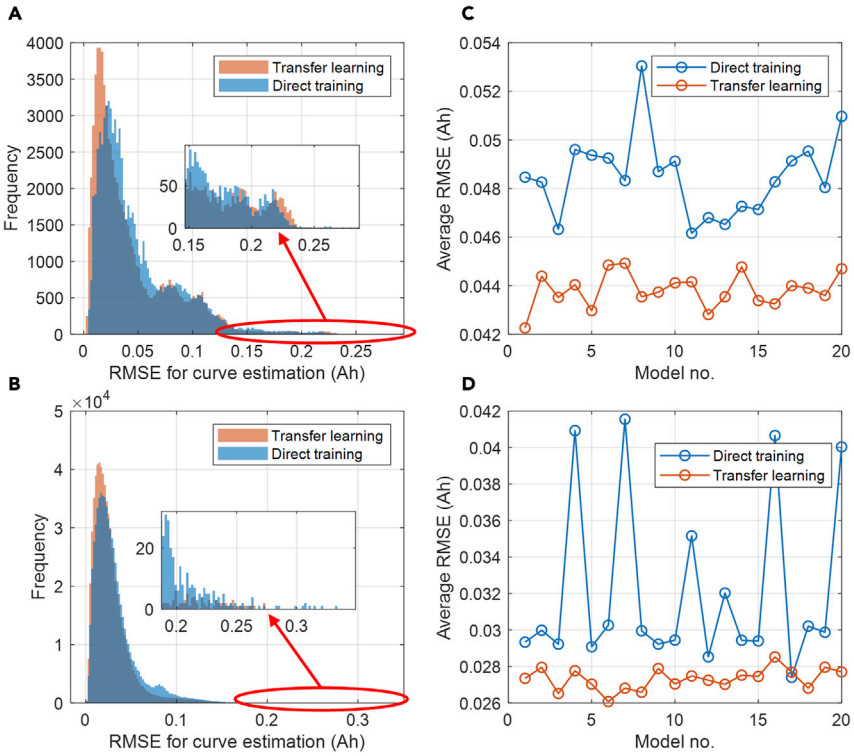

Figure 6. Charging curve estimation error using transfer learning and direct training.

(A and B) The RMSE for curve estimation based on transfer-learning and direct-training approaches: (A) NASA dataset. (B) CALCE dataset. Each subplot summarizes test results from 20 DNNs trained independently.

(C and D) The average RMSE of the 20 DNNs based on direct training and transfer learning, respectively: (C) NASA dataset. (D) CALCE dataset.

Limitations and outlook

The present study can be improved in the future. First, this study only involves the widely used constant-current charging data for commercial batteries. As a data-driven approach, the proposed method does not assume a specific charging strategy or battery materials. Thus, the proposed method can be explored to apply to more diverse battery chemistries and different charging protocols.[11] Second, the proposed method can also be explored to predict dynamic characteristics of batteries under varying loads, as battery voltage and degradation show strong dependence on the working loads.[48] Finally, the present method only learns from experimental data while ignoring intrinsic aging mechanisms. As illustrated by Dubarry et al.,[49] open-circuit voltage characteristics over battery life can be clearly described by a physical model involving four parameters. The incorporation of deep-learning techniques and physical models might lead to more accurate and reliable prediction results.[50]

DISCUSSION

In this paper, we develop a DNN to estimate the entire charging curves of lithium-ion batteries by using a portion of the charging curves as the input. The entire charging curve depicts the capacity as a function of battery voltage. We demonstrate that the proposed method can accurately estimate the charging curves with a RMSE of less than 16.9 mAh for 0.74 Ah batteries using only a 300-mV piece of the charging curve.

From the estimated curves, we demonstrate that the key battery states like capacity and energy can be accurately extracted once the charging voltage is measured. Maximum capacity and energy are estimated as the two examples of charging-curve estimation, and the influence of the input length is also discussed. Thus, our method addresses the estimation issue of multiple states over battery life. Even the IC curves can be derived from the estimated curves, enabling further analysis of battery internal aging mechanisms. The developed DNN can quickly adapt to different batteries working under different conditions. We show that the DNN developed by transfer learning can be more accurate and reliable than a completely new one, which enables the quick development of an accurate DNN for different batteries and is an effective approach for saving both cost and time.

To our knowledge, this is the first work to achieve accurate and comprehensive state estimation over battery life via reconstructing the constant-current charging curves. Our work shows the potentiality of deep learning to infer more comprehensive battery states. In the future, the present work will be extended to estimate and forecast more in-depth battery-aging information, including open-circuit voltage and impedance spectra at electrode levels.

EXPERIMENTAL PROCEDURES

Resource availability

Lead contact

Further information and requests for resources should be directed to and will be fulfilled by the lead contact, Prof. Dr. Rui Xiong (rxiong@bit.edu.cn).

Materials availability

This study did not generate new unique materials.

Data and code availability

The data and code that support the findings of this study are available at https://github.com/aesabattery/Charging-Curve-Prediction.

DNN training

The developed DNN is depicted in Figure 7. It consists primarily of four kinds of layers: the 1D convolutional, maximum pooling, dense and dropout layers. A 1D convolutional layer incorporates a few filters, each of which outputs its dot product between the input data in a given window and its weights. The window moves along the input to condense information. In the designed DNN, the numbers of filters are 16, 8 and 8 for the three convolutional layers in sequence, respectively. We set the window size to be 3, and the window moves at a step of 1. The causal padding and the rectified linear unit (ReLU) activation function are applied as well. The maximum pooling layers are incorporated following the convolutional layers. In the first two maximum pooling layers, the maximum element is extracted from its input over a given pool size of 3. Following the final 1D convolutional layer is a global maximum pooling layer whose pool size is equal to its input size. Afterwards, a dense layer is concatenated, and the number of neurons in this layer is 140. The neurons in a dense layer output the dot product between input and weights and then feed them into the ReLU activation function. It is followed by a dropout layer which randomly disables 20% input units by setting them to 0. The final layer is also a dense layer whose size coincides with the length of the regression target. In this layer, no activation function is employed, and it outputs the estimation results.

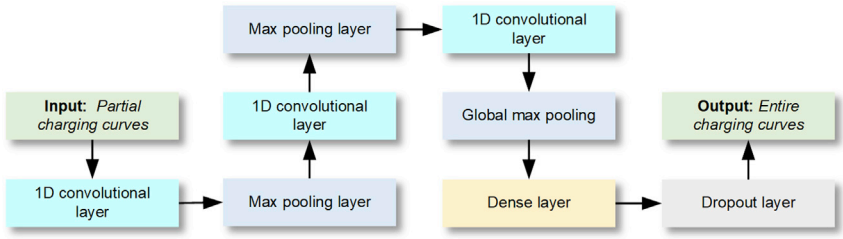

Figure 7. The architecture of the developed DNN

The DNN is trained by Adam algorithm.[51] The input data are normalized as $x_n = \frac{x-\mu}{\sigma}$ before being fed into the DNNs, and x and x_n represent the raw and normalized input data, respectively. μ and σ are the mean and standard deviation computed using x from the training dataset, respectively. The batch size is 400. The loss function is the mean squared error of the charging curves. During the training process, 35% of the training samples are randomly selected and left aside to form a validation dataset, based on which the validation loss is computed. The DNN is trained for the maximum number of 50,000 epochs and the DNN with the minimum validation loss is picked up as the final model.

Transfer learning

Transfer learning aims to facilitate the development of a DNN for curve estimation of new batteries working at different scenarios using a pre-trained DNN. In this regard, the final output layer of a pre-trained DNN is replaced by a new dense layer with the number of neurons corresponding to the length of the regression target. When implementing the DNN, the charging curves are scaled down according to battery nominal capacities. The modified DNN is firstly trained for 50 epochs with only the final layer trainable. Afterward, all layers are trained for another 4,950 epochs. In contrast, a new DNN with the same structure is developed and trained for the maximum number of 5,000 epochs in the same way as developing the pre-trained DNN.

The development of all DNNs is implemented in the Keras Python library with a TensorFlow backend (version 2.4.3)[52] and the computation is executed based on a Tesla V100-DGXS-32GB graphics processing unit (GPU).

SUPPLEMENTAL INFORMATION

Supplemental information can be found online at https://doi.org/10.1016/j.joule.2021.05.012.

ACKNOWLEDGMENTS

R.X. acknowledges the financial support from National Natural Science Foundation of China (51922006 and 51877009).

AUTHOR CONTRIBUTIONS

J.T. and R.X. conceived the study. J.T. and J.L. collected data and developed algorithms. J.T. and R.X. wrote the first draft of the manuscript. W.S. and X.-G.Y. edited the manuscript. All authors contributed to analysis of the results.

DECLARATION OF INTERESTS

The authors have applied for a patent related to this work.

Received: February 12, 2021
Revised: March 31, 2021
Accepted: May 13, 2021
Published: June 16, 2021

REFERENCES

1. Palacín, M.R. (2018). Understanding ageing in Li-ion batteries: a chemical issue. Chem. Soc. Rev. *47*, 4924–4933.
2. Palacín, M.R., and de Guibert, A. (2016). Why do batteries fail? Science *351*, 1253292.
3. Barai, A., Uddin, K., Dubarry, M., Somerville, L., McGordon, A., Jennings, P., and Bloom, I. (2019). A comparison of methodologies for the non-invasive characterisation of commercial Li-ion cells. Prog. Energy Combust. Sci. *72*, 1–31.
4. Song, L., Zhang, K., Liang, T., Han, X., and Zhang, Y. (2020). Intelligent state of health estimation for lithium-ion battery pack based on big data analysis. J. Energy Storage *32*, 101836.
5. Tian, J., Xiong, R., and Shen, W. (2019). A review on state of health estimation for lithium ion batteries in photovoltaic systems. eTransportation *2*, 100028.
6. Li, Y., Liu, K., Foley, A.M., Zülke, A., Berecibar, M., Nanini-Maury, E., Van Mierlo, J., and Hoster, H.E. (2019). Data-driven health estimation and lifetime prediction of lithium-ion batteries: a review. Renew. Sustain. Energy Rev. *113*, 109254.
7. Ng, M., Zhao, J., Yan, Q., Conduit, G.J., and Seh, Z.W. (2020). Predicting the state of charge and health of batteries using data-driven machine learning. Nat. Mach. Intell. *2*, 161–170.
8. Zhang, Y., Tang, Q., Zhang, Y., Wang, J., Stimming, U., and Lee, A.A. (2020). Identifying degradation patterns of lithium ion batteries from impedance spectroscopy using machine learning. Nat. Commun. *11*, 1706.
9. Severson, K.A., Attia, P.M., Jin, N., Perkins, N., Jiang, B., Yang, Z., Chen, M.H., Aykol, M., Herring, P.K., Fraggedakis, D., et al. (2019). Data-driven prediction of battery cycle life before capacity degradation. Nat. Energy *4*, 383–391.
10. Andre, D., Meiler, M., Steiner, K., Wimmer, C., Soczka-Guth, T., and Sauer, D.U. (2011). Characterization of high-power lithium-ion batteries by electrochemical impedance spectroscopy. I. Experimental investigation. J. Power Sources *196*, 5334–5341.
11. Tomaszewska, A., Chu, Z., Feng, X., O'Kane, S., Liu, X., Chen, J., Ji, C., Endler, E., Li, R., Liu, L., et al. (2019). Lithium-ion battery fast charging: a review. eTransportation *1*, 100011.
12. Sugiyama, M., Krauledat, M., and Müller, K.R. (2007). Covariate shift adaptation by importance weighted cross validation. J. Mach. Learn. Res. *8*, 985–1005.
13. Weng, C., Cui, Y., Sun, J., and Peng, H. (2013). On-board state of health monitoring of lithium-ion batteries using incremental capacity analysis with support vector regression. J. Power Sources *235*, 36–44.
14. Khaleghi, S., Firouz, Y., Berecibar, M., Mierlo, J.V., and Bossche, P.V.D. (2020). Ensemble gradient boosted tree for SoH estimation based on diagnostic features. Energies *13*, 1262.
15. Richardson, R.R., Birkl, C.R., Osborne, M.A., and Howey, D.A. (2019). Gaussian process regression for in situ capacity estimation of lithium-ion batteries. IEEE Trans. Ind. Inform. *15*, 127–138.
16. Li, Y., Zou, C., Berecibar, M., Nanini-Maury, E., Chan, J.C.-W., van den Bossche, P., Van Mierlo, J., and Omar, N. (2018). Random forest regression for online capacity estimation of lithium-ion batteries. Appl. Energy *232*, 197–210.
17. Zheng, Y., Ouyang, M., Han, X., Lu, L., and Li, J. (2018). Investigating the error sources of the online state of charge estimation methods for lithium-ion batteries in electric vehicles. J. Power Sources *377*, 161–188.
18. Zhang, Y., Xiong, R., He, H., and Shen, W. (2017). Lithium-ion battery pack state of charge and state of energy estimation algorithms using a hardware-in-the-loop validation. IEEE Trans. Power Electron *32*, 4421–4431.
19. Jiang, B., Dai, H., Wei, X., and Xu, T. (2019). Joint estimation of lithium-ion battery state of charge and capacity within an adaptive variable multi-timescale framework considering current measurement offset. Appl. Energy *253*, 113619.
20. Wang, Y., Zhang, C., and Chen, Z. (2014). A method for joint estimation of state-of-charge and available energy of LiFePO4 batteries. Appl. Energy *135*, 81–87.
21. Chen, C., Xiong, R., Yang, R., Shen, W., and Sun, F. (2019). State-of-charge estimation of lithium-ion battery using an improved neural network model and extended Kalman filter. J. Clean. Prod. *234*, 1153–1164.
22. Mulleriyawage, U.G.K., and Shen, W.X. (2020). Optimally sizing of battery energy storage capacity by operational optimization of residential PV-battery systems: an Australian household case study. Renew. Energy *160*, 852–864.
23. Lee, C.H., and Wu, C.H. (2015). A novel big data modeling method for improving driving range estimation of EVs. IEEE Access *3*, 1980–1993.
24. Dong, G., Chen, Z., Wei, J., Zhang, C., and Wang, P. (2016). An online model-based method for state of energy estimation of lithium-ion batteries using dual filters. J. Power Sources *301*, 277–286.
25. Lai, X., He, L., Wang, S., Zhou, L., Zhang, Y., Sun, T., and Zheng, Y. (2020). Co-estimation of state of charge and state of power for lithium-ion batteries based on fractional variable-order model. J. Clean. Prod. *255*, 120203.
26. Fly, A., and Chen, R. (2020). Rate dependency of incremental capacity analysis (dQ/dV) as a diagnostic tool for lithium-ion batteries. J. Energy Storage *29*, 101329.
27. Dost, P., Spichartz, P., and Sourkounis, C. (2015). Charging behaviour of users utilising battery electric vehicles and extended range electric vehicles within the scope of a field test. 2015 International conference Renewable Energy Research Appliance ICRERA, pp. 1162–1167.
28. Birkl, C. (2017). Oxford Battery Degradation Dataset 1.doi:10.5287/bodleian:KO2kdmYGg
29. Dubarry, M., Truchot, C., and Liaw, B.Y. (2012). Synthesize battery degradation modes via a diagnostic and prognostic model. J. Power Sources *219*, 204–216.
30. Dubarry, M., Svoboda, V., Hwu, R., and Yann Liaw, B. (2006). Incremental capacity analysis and close-to-equilibrium OCV measurements to quantify capacity fade in commercial rechargeable lithium batteries. Electrochem. Solid-State Lett. *9*, A454.
31. Han, X., Ouyang, M., Lu, L., Li, J., Zheng, Y., and Li, Z. (2014). A comparative study of commercial lithium ion battery cycle life in electrical vehicle: aging mechanism identification. J. Power Sources *251*, 38–54.
32. Berecibar, M., Gandiaga, I., Villarreal, I., Omar, N., Van Mierlo, J., and Van Den Bossche, P. (2016). Critical review of state of health estimation methods of Li-ion batteries for real applications. Renew. Sustain. Energy Rev. *56*, 572–587.
33. Farmann, A., Waag, W., Marongiu, A., and Sauer, D.U. (2015). Critical review of on-board capacity estimation techniques for lithium-ion batteries in electric and hybrid electric vehicles. J. Power Sources *281*, 114–130.
34. Weng, C., Feng, X., Sun, J., and Peng, H. (2016). State-of-health monitoring of lithium-ion battery modules and packs via incremental capacity peak tracking. Appl. Energy *180*, 360–368.

35. Tian, J., Xiong, R., Shen, W., and Lu, J. (2021). State-of-charge estimation of LiFePO4 batteries in electric vehicles: A deep-learning enabled approach. Appl. Energy *291*, 116812.

36. Ouyang, M., Liu, G., Lu, L., Li, J., and Han, X. (2014). Enhancing the estimation accuracy in low state-of-charge area: A novel onboard battery model through surface state of charge determination. J. Power Sources *270*, 221–237.

37. Li, K., and Tseng, K.J. (2015). Energy efficiency of lithium-ion battery used as energy storage devices in micro-grid. IECON 2015 - 41st Annual Conference of the IEEE Industrial Electronics Society, pp. 5235–5240.

38. Yang, X.-G., Liu, T., Gao, Y., Ge, S., Leng, Y., Wang, D., and Wang, C.-Y. (2019). Asymmetric temperature modulation for extreme fast charging of lithium-ion batteries. Joule *3*, 3002–3019.

39. Pan, S.J., and Yang, Q. (2010). A survey on transfer learning. IEEE Trans. Knowl. Data Eng. *22*, 1345–1359.

40. Bole, B., Kulkarni, C., and Daigle, M. (2014). Randomized battery usage data set. NASA AMES Progn. data Repos, 70. https://ti.arc.nasa.gov/tech/dash/groups/pcoe/prognostic-data-repository/#batteryrnddischarge.

41. Bole, B., Kulkarni, C., and Daigle, M. (2014). Adaptation of an electrochemistry-based Li-ion battery model to account for deterioration observed under randomized use. Annual conference of the prognostics and health management society *2014*, 502–510.

42. Xing, Y., Ma, E.W.M., Tsui, K.L., and Pecht, M. (2013). An ensemble model for predicting the remaining useful performance of lithium-ion batteries. Microelectron. Reliab. *53*, 811–820.

43. He, W., Williard, N., Osterman, M., and Pecht, M. (2011). Prognostics of lithium-ion batteries based on Dempster-Shafer theory and the Bayesian Monte Carlo method. J. Power Sources *196*, 10314–10321.

44. Yang, X.-G., Leng, Y., Zhang, G., Ge, S., and Wang, C.-Y. (2017). Modeling of lithium plating induced aging of lithium-ion batteries: transition from linear to nonlinear aging. J. Power Sources *360*, 28–40.

45. Tan, B., Zhang, Y., Pan, S., and Yang, Q. (2017). Distant domain transfer learning. Proceedings of the AAAI conference on artificial intelligence, pp. 2604–2610.

46. Li, W., Rentemeister, M., Badeda, J., Jöst, D., Schulte, D., and Sauer, D.U. (2020). Digital twin for battery systems: cloud battery management system with online state-of-charge and state-of-health estimation. J. Energy Storage *30*, 101557.

47. Wu, B., Widanage, W.D., Yang, S., and Liu, X. (2020). Battery digital twins: perspectives on the fusion of models, data and artificial intelligence for smart battery management systems. Energy and AI *1*, 100016.

48. Raj, T., Wang, A.A., Monroe, C.W., and Howey, D.A. (2020). Investigation of path-dependent degradation in lithium-ion batteries. Batteries & Supercaps *3*, 1377–1385.

49. Dubarry, M., and Beck, D. (2020). Big data training data for artificial intelligence-based Li-ion diagnosis and prognosis. J. Power Sources *479*, 228806.

50. Aykol, M., Gopal, C.B., Anapolsky, A., Herring, P.K., van Vlijmen, B., Berliner, M.D., Bazant, M.Z., Braatz, R.D., Chueh, W.C., and Storey, B.D. (2021). Perspective—combining physics and machine learning to predict battery lifetime. J. Electrochem. Soc. *168*, 030525.

51. Kingma, D.P., and Ba, J. (2014). Adam: a method for stochastic optimization (3rd International Conference for Learning Representations), pp. 1–15.

52. Chollet, F., et al.. https://keras.io.